JCI The Journal of Clinical Investigation

AMPK dysregulation promotes diabetes-related reduction of superoxide and mitochondrial function

Laura L. Dugan, … , Robert K. Naviaux, Kumar Sharma

J Clin Invest. 2013;123(11):4888-4899. https://doi.org/10.1172/JCI66218.

Research Article

Diabetic microvascular complications have been considered to be mediated by a glucose-driven increase in mitochondrial superoxide anion production. Here, we report that superoxide production was reduced in the kidneys of a steptozotocin-induced mouse model of type 1 diabetes, as assessed by in vivo real-time transcutaneous fluorescence, confocal microscopy, and electron paramagnetic resonance analysis. Reduction of mitochondrial biogenesis and phosphorylation of pyruvate dehydrogenase (PDH) were observed in kidneys from diabetic mice. These observations were consistent with an overall reduction of mitochondrial glucose oxidation. Activity of AMPK, the major energy-sensing enzyme, was reduced in kidneys from both diabetic mice and humans. Mitochondrial biogenesis, PDH activity, and mitochondrial complex activity were rescued by treatment with the AMPK activator 5-aminoimidazole-4-carboxamide-1-β-D-ribofuranoside (AICAR). AICAR treatment induced superoxide production and was linked with glomerular matrix and albuminuria reduction in the diabetic kidney. Furthermore, diabetic heterozygous superoxide dismutase 2 (*Sod2*$^{+/-}$) mice had no evidence of increased renal disease, and *Ampka2*$^{-/-}$ mice had increased albuminuria that was not reduced with AICAR treatment. Reduction of mitochondrial superoxide production with rotenone was sufficient to reduce AMPK phosphorylation in mouse kidneys. Taken together, these results demonstrate that diabetic kidneys have reduced superoxide and mitochondrial biogenesis and activation of AMPK enhances superoxide production and mitochondrial function while reducing disease activity.

 Related Commentary, page 4573

AMPK dysregulation promotes diabetes-related reduction of superoxide and mitochondrial function

Laura L. Dugan,[1] Young-Hyun You,[2,3] Sameh S. Ali,[1] Maggie Diamond-Stanic,[2,3] Satoshi Miyamoto,[2,3] Anne-Emilie DeCleves,[2,3] Aleksander Andreyev,[4] Tammy Quach,[2,3] San Ly,[2,3] Grigory Shekhtman,[1] William Nguyen,[1] Andre Chepetan,[1] Thuy P. Le,[5] Lin Wang,[5] Ming Xu,[5] Kacie P. Paik,[5] Agnes Fogo,[6] Benoit Viollet,[7] Anne Murphy,[4] Frank Brosius,[8] Robert K. Naviaux,[5] and Kumar Sharma[2,3]

[1]Division of Geriatrics, Department of Medicine, and [2]Center for Renal Translational Medicine, Division of Nephrology-Hypertension, Department of Medicine, UCSD, La Jolla, California, USA. [3]Veterans Administration San Diego Healthcare System, La Jolla, California, USA. [4]Department of Pharmacology and [5]The Mitochondrial and Metabolic Disease Center, Departments of Medicine, Pediatrics, and Pathology, UCSD, La Jolla, California, USA. [6]Department of Pathology, Vanderbilt University, Nashville, Tennessee, USA. [7]Institut Cochin, Université Paris Descartes, CNRS (UMR 8104), Paris, France. [8]Department of Internal Medicine, University of Michigan Medical School, Ann Arbor, Michigan, USA.

Diabetic microvascular complications have been considered to be mediated by a glucose-driven increase in mitochondrial superoxide anion production. Here, we report that superoxide production was reduced in the kidneys of a steptozotocin-induced mouse model of type 1 diabetes, as assessed by in vivo real-time transcutaneous fluorescence, confocal microscopy, and electron paramagnetic resonance analysis. Reduction of mitochondrial biogenesis and phosphorylation of pyruvate dehydrogenase (PDH) were observed in kidneys from diabetic mice. These observations were consistent with an overall reduction of mitochondrial glucose oxidation. Activity of AMPK, the major energy-sensing enzyme, was reduced in kidneys from both diabetic mice and humans. Mitochondrial biogenesis, PDH activity, and mitochondrial complex activity were rescued by treatment with the AMPK activator 5-aminoimidazole-4-carboxamide-1-β-D-ribofuranoside (AICAR). AICAR treatment induced superoxide production and was linked with glomerular matrix and albuminuria reduction in the diabetic kidney. Furthermore, diabetic heterozygous superoxide dismutase 2 (*Sod2*$^{+/-}$) mice had no evidence of increased renal disease, and *Ampka2*$^{-/-}$ mice had increased albuminuria that was not reduced with AICAR treatment. Reduction of mitochondrial superoxide production with rotenone was sufficient to reduce AMPK phosphorylation in mouse kidneys. Taken together, these results demonstrate that diabetic kidneys have reduced superoxide and mitochondrial biogenesis and activation of AMPK enhances superoxide production and mitochondrial function while reducing disease activity.

Introduction

Complications of diabetes, including retinopathy, neuropathy, and nephropathy, are responsible for considerable morbidity, and are experienced by a majority of individuals with diabetes over time. How elevated glucose levels initiate these complications remains unclear. The prevailing theory states that enhanced mitochondrial production of superoxide anion in response to elevated cellular glucose concentrations leads to pathological pathway activation and cell dysfunction (1, 2). Studies in cell culture systems demonstrated that addition of high glucose produced an increase in ROS that has been attributed to the mitochondrial electron transport chain (ETC). The currently accepted scheme is that chronically elevated glucose leads to increased ROS production by mitochondria, contributing to downstream cellular injury processes, and ultimately resulting in end-organ dysfunction and structural changes. Based on this theory, numerous strategies are being developed to interrupt the mitochondrial production of superoxide and inhibit downstream deleterious pathways.

Definitive data to support this theory and demonstrate that superoxide anion production is indeed stimulated in diabetic organs in vivo, however, is lacking. Although several groups have identified markers of oxidative stress and oxidative damage in diabetic kidneys or kidney cells (3, 4), no studies to date have attempted to measure and quantify superoxide production with diabetes directly in vivo. As the half-life of superoxide anion in cells is measured in seconds and it is rapidly converted to hydrogen peroxide and other reactive oxygen intermediates, the measurement of superoxide production has been challenging (5), especially in the intact organism. As the tissue response to elevated glucose concentrations in vivo may differ from the response in cell cultures, we carried out in vivo studies to evaluate the production of superoxide anion in the kidney in chronically diabetic mice. Because of the difficulties inherent in following superoxide production, multiple methods of measuring this short-lived radical were utilized in the current study, all of which produced confirmatory results.

Results

Diabetic mice have reduced renal superoxide production. Male C57BL/6J mice made diabetic by multiple low-dose injections of streptozotocin (STZ) showed significantly elevated plasma glucose concentrations 4 weeks after onset of hyperglycemia (Supplemental

Authorship note: Laura L. Dugan and Young-Hyun You contributed equally to this work.

Conflict of interest: Kumar Sharma and Robert K. Naviaux have equity interest in ClinMet Inc.

Citation for this article: *J Clin Invest.* 2013;123(11):4888–4899. doi:10.1172/JCI66218.

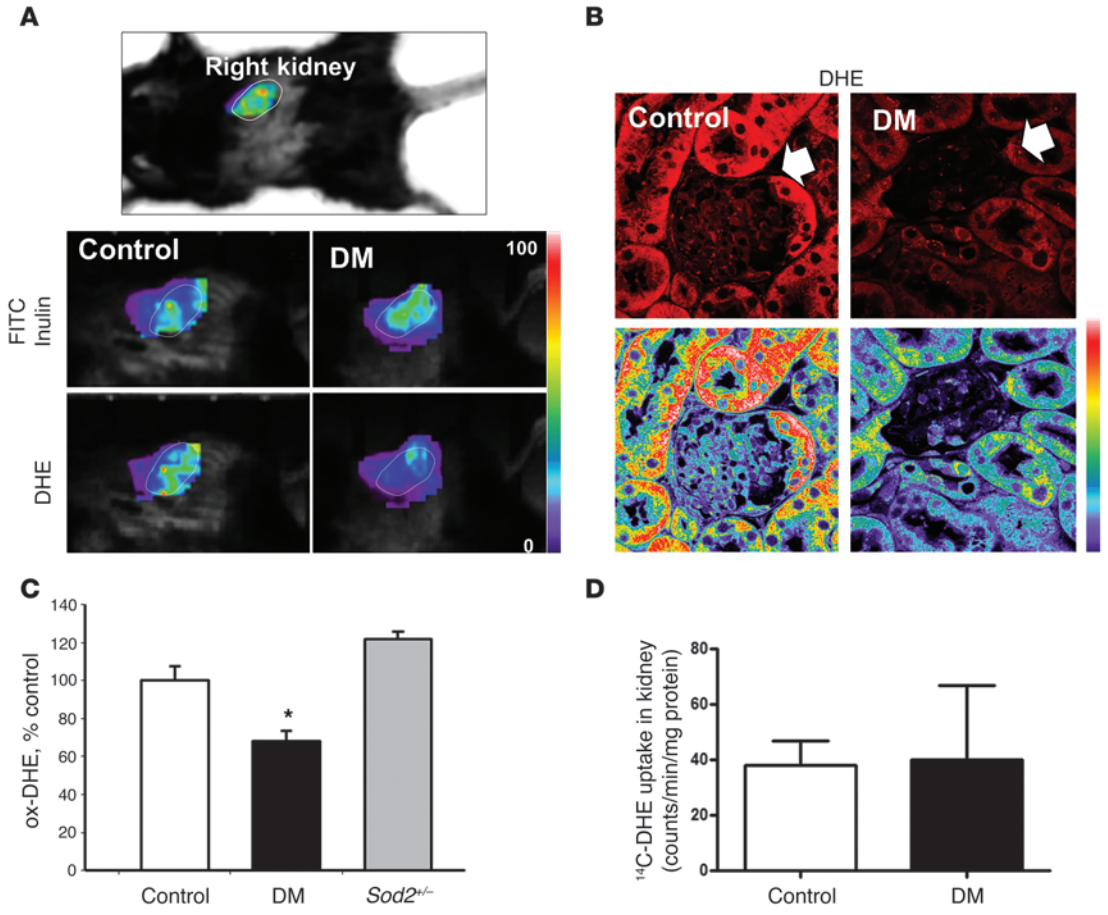

Figure 1

Imaging of kidney superoxide production in normal and diabetic mice. (**A**) Live animal imaging of kidney through the intact skin in a prone, isofluorane-anesthetized mouse. Kidneys were first localized using the FITC channel, and then the filter settings were changed to the ox-DHE channel (Ex 470 nm, EM > 590 nm) to image superoxide production in control and STZ-induced diabetic mice (DM). Fluorescence is shown using a linear pseudocolor scale (images representative of $n = 6$ mice per group). Original magnification, ×1 (top panel); ×1.25 (bottom panels). (**B**) ox-DHE fluorescence (red, top; linear pseudocolor, bottom) in kidney slices prepared from DHE-injected control and DM mice with less in vivo oxidation in DM kidney. Diabetic kidneys had a reduced level of glomerular DHE oxidation-derived fluorescence (white arrow). Original magnification, ×63. (**C**) Kidneys from *Sod2*$^{+/-}$ mice, which are deficient in mitochondrial SOD, were evaluated and demonstrated the expected higher superoxide than controls. $n \geq 15$ each for control and diabetic groups, $n = 3$ for *Sod2*$^{+/-}$ group, $^*P < 0.05$ vs control. (**D**) In vivo analysis of [^{14}C]-labeled DHE with STZ-diabetic mice and control mice.

Table 1; supplemental material available online with this article; doi:10.1172/JCI66218DS1). Real-time superoxide production in kidney was measured using systemic administration of dihydroethidium (DHE) to detect superoxide (Figure 1A), using a method recently described for real-time imaging of superoxide anion production in brain (6). To identify the position of the kidneys in the intact animal, control and diabetic mice were coinjected with FITC-inulin 30 minutes prior to being placed in the scanner. FITC-inulin is filtered by the kidney, allowing the location of the kidneys to be established by visualizing the FITC signal (Figure 1A). The optical settings on the scanner were then changed to detect the DHE oxidation product (Ex 488 nm, Em > 590 nm), and the region over the kidney was imaged (circled). DHE oxidation was prominent in normal kidneys, but surprisingly, diabetic kidneys had reduced DHE oxidation, indicating reduced superoxide production.

To evaluate specific tissue compartments, mice underwent administration of DHE 16 hours prior to euthanasia at which time kidneys were then harvested (7, 8), a point at which all unreacted DHE had been excreted (6). Confocal imaging of slices prepared from animals injected with DHE also demonstrated that control mice had significantly higher superoxide production in kidney cortex than diabetic animals (Figure 1, B and C). The DHE oxidation was reduced in the glomeruli and podocytes of the diabetic kidneys (Supplemental Figure 1A). Mice made diabetic with Akita (in C57BL/6J and an F1 cross with DBA2J and C57BL/6J with Akita, F1[DBA/2J × C57BL/6J] – *Ins2Akita*) were also found to have reduced DHE fluorescence in the kidney, heart, and liver (Supplemental Figure 1, B–G). These data demonstrate that the kidney from multiple models of type 1 diabetes exhibits lower, not higher, superoxide production than normal kidneys.

To confirm that increased mitochondrial superoxide production, if present, could in fact be visualized by our in vivo DHE method, mice that were heterozygous for the mitochondrial superoxide dismutase 2 (Sod2; *Sod2*$^{+/-}$ mice) and that had known elevation of mitochondrial superoxide were imaged. *Sod2*$^{+/-}$ mice exhibited the expected increase in DHE oxidation (Figure 1C and see

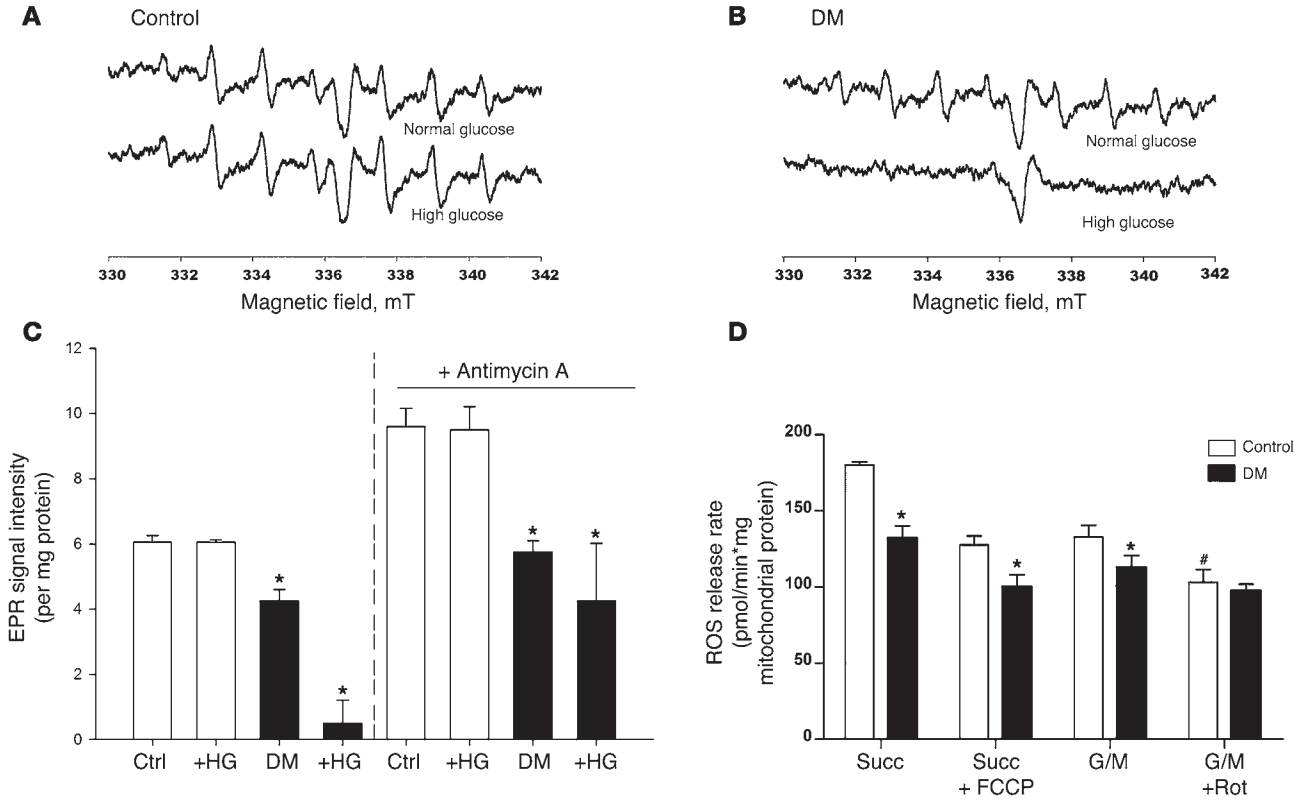

Figure 2

EPR spectra and ROS release rate in control and diabetic kidney mitochondria. Dissociated kidney cell suspensions from control (**A**) or diabetic (**B**) animals were prepared as described and analyzed by EPR using DPMPO as the spin probe 10 minutes after addition of the mitochondrial substrates malate and pyruvate. The characteristic spectrum for the superoxide-DPMPO was observed in both control and diabetic samples at baseline. However, addition of high glucose (bottom traces) did not increase mitochondrial superoxide production and, in the diabetic kidney samples, actually reduced superoxide production. (**C**) Analysis of the EPR signal intensity using the upfield peak at 334 mT, normalized to mg protein. Values are mean ± SEM, $n = 6$ per condition, $^{*}P < 0.05$ vs control. The second set of bars to the right show data derived from Supplemental Figure 3, which shows additional spectra from samples after addition of the mitochondrial complex III inhibitor, antimycin A. Antimycin A produced the expected increase in superoxide, confirming the ability of this technique to detect increased mitochondrial superoxide production if present. (**D**) Decreased ROS release from kidney mitochondria isolated from diabetic animals Measurements were made in the presence of succinate (Succ), succinate and FCCP (Succ + FCCP), glutamate plus malate (G/M) or glutamate plus malate with rotenone (G/M + Rot) by Amplex Red assay. Rates were calculated using calibration curve as described in Methods. Values are mean ± SEM, $n = 5–8$. $^{*}P < 0.001$ vs. corresponding control; $^{\#}P < 0.05$ vs. G/M.

below). It is possible that the reduction in DHE fluorescence could be due to altered excretion of DHE in diabetic mice. To assure that uptake of DHE was the same in control and diabetic kidneys, [^{14}C]-labeled DHE was synthesized and administered to the normal control and diabetic mice. The amount of [^{14}C]-labeled DHE was the same ($P = 0.96$) in the normal and diabetic kidney (Figure 1D). Additional validation of the in vivo DHE imaging as a specific approach to in vivo superoxide anion detection was recently demonstrated using time domain fluorescence lifetime deconvolution of live images, LC-mass spectroscopy, and electrochemical analyses of DHE/oxidation products in tissues from DHE-injected mice (6).

We then directly measured mitochondrial production of superoxide anion ex vivo from kidney cortical homogenates of control and diabetic animals via electron paramagnetic resonance (EPR) (refs. 9–15; Figure 2). 5-(diethoxyphosphoryl)-5-methyl-1-pyrroline-N-oxide (DEPMPO) was used as the spin-trap because of the long half-life of the DMPPO-superoxide adduct (DEPMPO-OOH). As expected, when the mitochondrial substrates malate, pyruvate, and ADP were added to the kidney tissue homogenates from either normal control or diabetic mice, there was an increase in superoxide production (Figure 2, A and B); however, there was no detectable increase in kidney homogenate from diabetic mice as compared with kidney homogenate from control mice. In contrast to the commonly held belief that high glucose will further increase superoxide production by mitochondria, direct addition of high glucose (25 mM) failed to produce an increase in superoxide levels in control homogenates and actually caused a decrease in superoxide production in diabetic homogenates (Figure 2, A and B). To verify that these findings were not simply due to loss of mitochondrial integrity in our preparations, at the end of each EPR study, the ETC complex III inhibitor antimycin A was added. In all preparations, antimycin A produced the expected large increase in mitochondrial superoxide production, thus confirming that increased mitochondrial superoxide flux could be detected, if present (Supplemental Figure 2, A and B). Additional control experiments in the presence of SOD completely elimi-

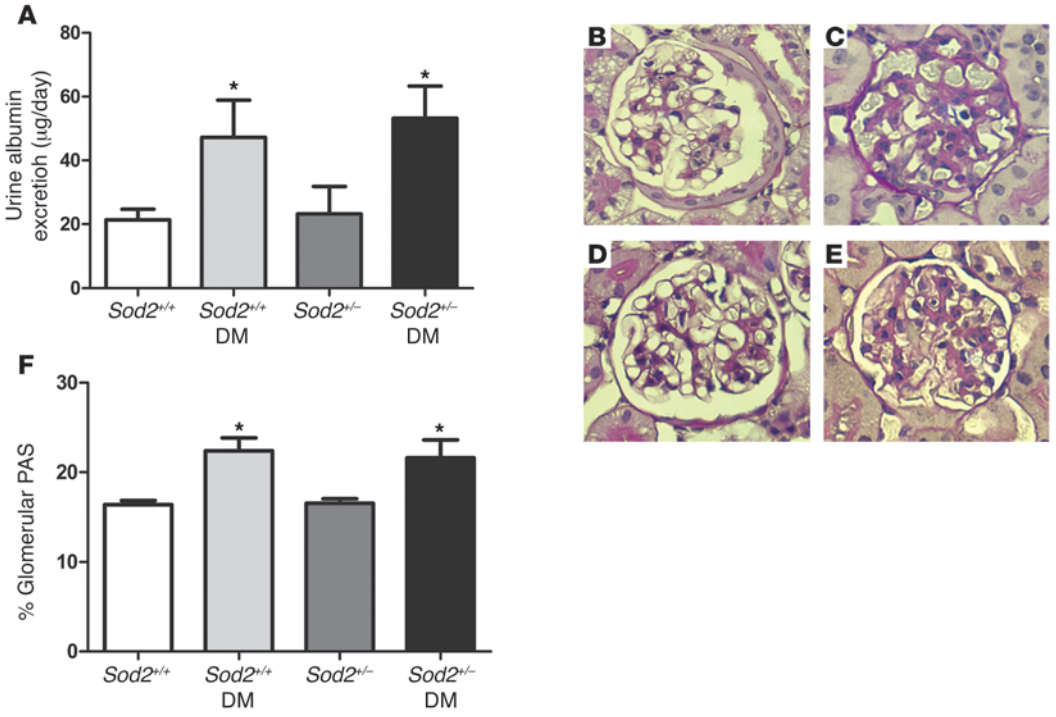

Figure 3
Diabetic kidney disease in *Sod2*$^{+/-}$ mice. (**A**) Albumin excretion for 24 hours, n = 9–10 each, *$P < 0.05$, compared with corresponding control group. Values are mean ± SEM. (**B**–**E**) PAS staining of (**B**) *Sod2*$^{+/+}$, (**C**) *Sod2*$^{+/+}$ diabetic, (**D**) *Sod2*$^{+/-}$, and (**E**) *Sod2*$^{+/-}$ diabetic mice. (**F**) Glomerular extracellular matrix expressed with percentage of the total glomerular area stained with PAS. n = 6–7. *$P < 0.001$, compared with corresponding control group. Original magnification, ×40.

nated the EPR signal of the spin trap-superoxide adduct, thus confirming the identity of the ROS being detected as the superoxide anion (data not shown). As an index of ROS production directly from mitochondria, isolated mitochondria from diabetic kidneys exhibited reduced production of hydrogen peroxide in response to mitochondrial substrates as compared with control mice (Figure 2D). However, measurement of hydrogen peroxide in the urine, glomerular 8-hydroxydeoxyguanosine (8-OHdG) staining, and nitrotyrosine staining from diabetic mice demonstrated a robust increase (see below), as previously described (16) thus demonstrating that some specific ROS moieties do increase in our diabetic models from nonmitochondrial sources, despite the lack of an overall mitochondrial superoxide anion increase.

To further evaluate a potential role for mitochondrial superoxide production, diabetes was induced in the *Sod2*$^{+/-}$ mice (Supplemental Table 2). The degree of hyperglycemia and body weight changes were similar in diabetic wild-type and *Sod2*$^{+/-}$ mice. It would be anticipated that the increase in mitochondrial superoxide in the *Sod2*$^{+/-}$ mice would exacerbate renal disease at baseline or with diabetes. However, there was no evidence of an increase in albuminuria or mesangial matrix expansion in the *Sod2*$^{+/-}$ mice with or without diabetes (Figure 3).

Diabetes is associated with increased mitochondrial DNA mutations and reduced mitochondrial biogenesis. As diabetes was characterized by reduced mitochondrial superoxide anion production, we examined parameters of mitochondrial structure and function in the normal and diabetic kidney. To assess mitochondria at a structural level, we developed a real-time quantitative PCR (qPCR) assay for the most commonly found mtDNA deletion in mice as a marker of mtDNA damage. This is called the D17 deletion and is located within the minor arc of murine mtDNA (Figure 4A). Diabetic mice had a 3-fold increase in mtDNA deletions in their kidneys (Figure 4B). A similar increase in renal mtDNA deletions was also found in kidneys of diabetic mice with F1(DBA/2 × C57BL/6) – *Ins*$^{2+/C96Y}$ Akita mutation (see below), indicating that STZ itself was not the basis for the increase in mtDNA deletions.

We hypothesized that an overall reduction in mitochondrial superoxide production could be due to a redistribution of carbons and electrons away from mitochondria and to the cytosol. The pyruvate dehydrogenase (PDH) complex is the major gateway for pyruvate carbons to enter the Krebs cycle in mitochondria (17). When the E1α subunit of PDH is phosphorylated on serine 293 (PDHE1α-pSer^{293}), the enzyme is inhibited. We found that PDH was indeed hyperphosphorylated in the kidneys of diabetic mice (Figure 4, C and D).

Gene expression and protein levels of PGC1α, the master regulator for mitochondrial biogenesis, were also reduced in the diabetic kidney (Figure 4E and Supplemental Figure 3A). The reduction of mitochondrial biogenesis and PGC1α in the diabetic kidney was postulated to be due to a reduction in activity of the master energy sensor, AMPK, based on recent studies demonstrating reduction of AMPK in states of caloric excess (16, 18, 19). Indeed, AMPK activity was reduced in the diabetic mouse kidney and glomeruli, as demonstrated by both immunostaining and a quantitative assay (Figure 4F and Supplemental Figure 3B). A similar process was demonstrated in humans, as immunostaining with a phosphorylated AMPK (p-AMPK) antibody indicated reduced AMPK activity in human diabetic nephropathy (Figure 4, G and H).

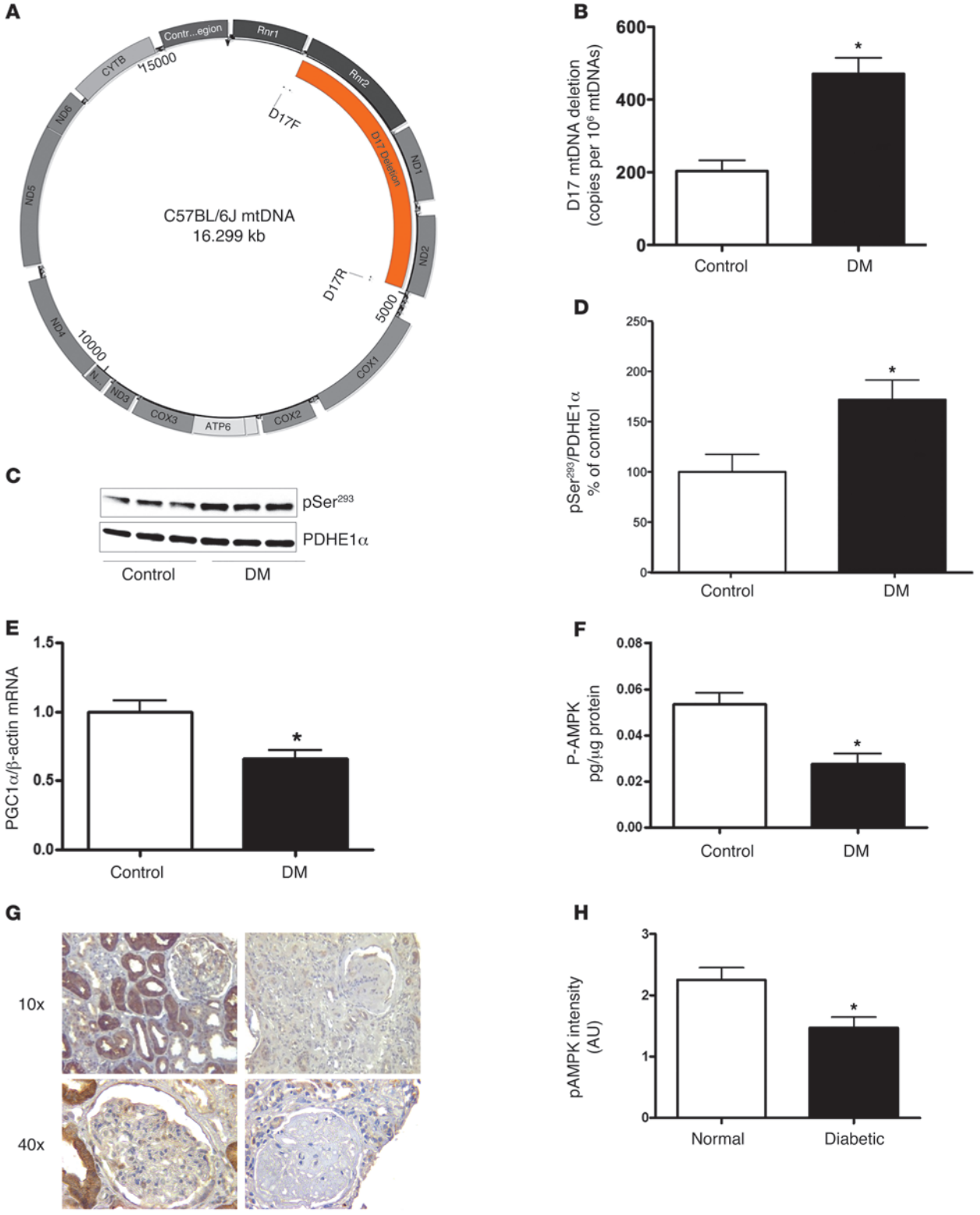
A
Contr...egion
Rnr1
Rnr2
CYTB
15000
D17F
D17 Deletion
ND6
ND1
ND5
C57BL/6J mtDNA
16.299 kb
ND2
D17R
5000
ND4
10000
COX1
ND3
COX3
ATP6
COX2
B
D17 mtDNA deletion (copies per 10^6 mtDNAs)
600
400
200
0
*
Control
DM
C
pSer293
PDHE1α
Control
DM
D
pSer293/PDHE1α % of control
250
200
150
100
50
0
*
Control
DM
E
PGC1α/β-actin mRNA
1.5
1.0
0.5
0.0
*
Control
DM
F
P-AMPK pg/μg protein
0.08
0.06
0.04
0.02
0.00
*
Control
DM
G
10x
40x
H
pAMPK intensity (AU)
3
2
1
0
*
Normal
Diabetic

Figure 4
Mitochondrial structure and function, PGC1α, and p-AMPK in the diabetic kidney. (**A**) Map of murine mtDNA indicating the location of the D17 deletion. (**B**) Quantitation of the D17 mtDNA deletion in kidney DNA from control and diabetic mice, (n = 6 per group, $^*P < 0.05$). (**C**) Representative immunoblot analysis of phosphorylated PDHE1α-pSer^{293} in kidney mitochondria (upper panel) and total PDHE1α (lower panel) from control and diabetic mice. (**D**) Quantitative analysis of the immunoblot results showing that, under conditions of diabetes, PDH is hyperphosphorylated (n = 6 per group, $^*P < 0.05$). (**E**) PGC1α is reduced in diabetic kidneys as demonstrated by real time PCR analysis of control and diabetic kidneys (n = 6 per group, $^*P < 0.05$) and immunofluorescence staining with an antibody to PGC1α in Supplemental Figure 2A. (**F**) p-AMPK was reduced in the diabetic kidneys, as demonstrated with an ELISA using kidney cortex from control and diabetic mice (n = 7 per group, $^*P < 0.05$) and with immunofluorescence staining with an antibody specific for p-Thr172 of the AMPKα subunit in Supplemental Figure 2B. (**G**) Representative images of immunostaining of p-AMPK in normal, diabetic kidney and negative control. Original magnification, ×40. (**H**) Semiquantitative scoring of p-AMPK intensity in glomeruli of human normal (n = 10) and diabetic kidney (n = 7 per group, $^*P < 0.05$).

To establish a link between reduced mitochondrial superoxide production and AMPK regulation, we administered rotenone to wild-type mice. Short-term rotenone has been previously demonstrated to reduce superoxide production (20, 21), and we found that rotenone administration led to a marked reduction in overall renal and heart DHE fluorescence consistent with a reduction in mitochondrial superoxide production (Figure 5, A and B). Although no effects were seen in blood glucose levels, rotenone reduced p-AMPK in both the kidney and heart (Figure 5, C–E, and G), indicating that reduced mitochondrial superoxide is sufficient to lower AMPK activity. Furthermore, rotenone administration led to an increase in p-PDH in both the kidney and heart (Figure 5, C, D, F, and H), which is consistent with reduced PDH activity and shunting away of pyruvate from the mitochondria in both these organs.

AMPK activation restores mitochondrial content and function and increases mitochondrial superoxide. To determine the role of AMPK activity in the regulation of mitochondrial content and function in the diabetic kidney, we administered 5-aminoimidazole-4-carboxamide-1-β-D-ribofuranoside (AICAR), an AMPK activator, to the diabetic mice for a period of 2 weeks. AICAR treatment in the type 1 diabetic mice did not lower blood glucose levels (Supplemental Table 1), but increased AMPK activity (Figure 6A) and restored PGC1α in the diabetic kidney (Figure 6B and see below). Superoxide production, as indicated by DHE oxidation, showed a significant increase in kidneys of STZ-induced diabetic mice treated with AICAR to levels similar to those of the nondiabetic mice (Figure 6, C and D). The Akita diabetic mouse also exhibited a reduction in DHE oxidation, which was restored by AMPK activation with AICAR (Figure 6, C and D). Overall mitochondrial protein content was reduced in the diabetic kidney and increased with AICAR (Figure 7A). Individual mitochondrial complex activity was measured from

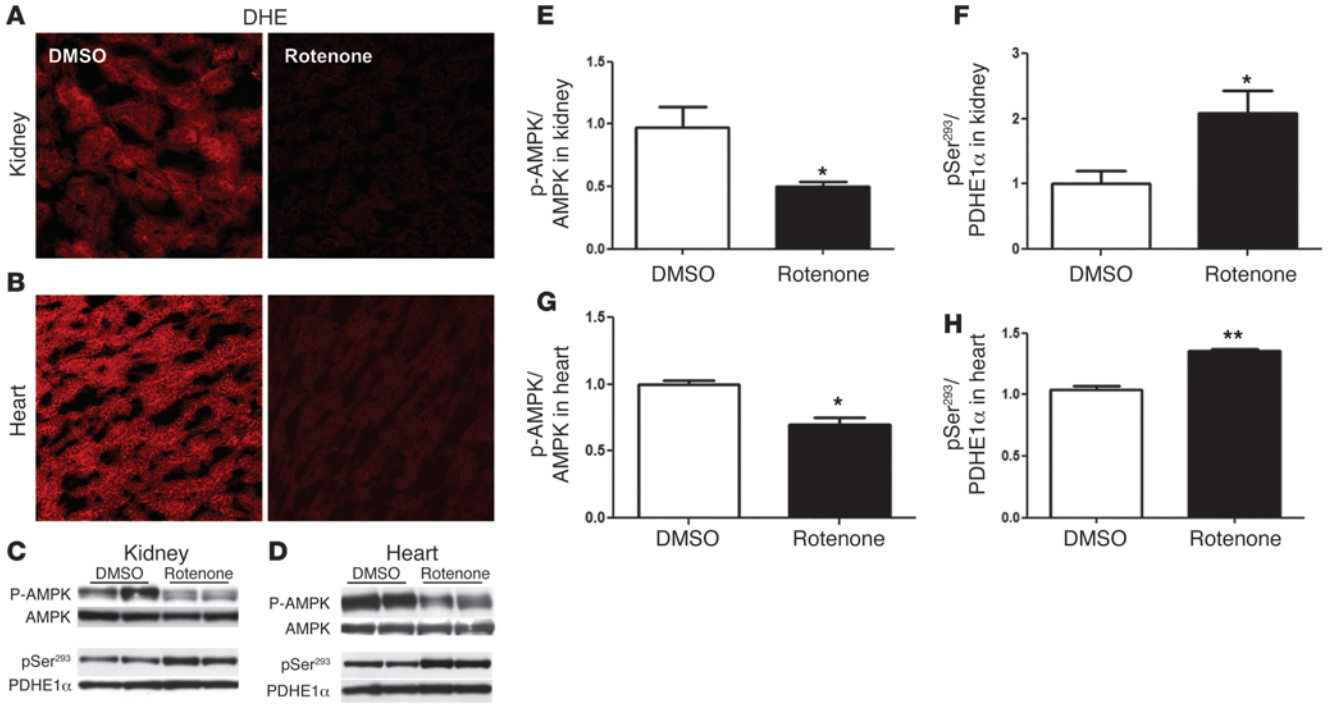

Figure 5
Rotenone reduces superoxide production in kidney and heart in association with reduced p-AMPK and increased p-PDH phosphorylation. C57BL/6J mice were injected i.p. with either 1 μg/g rotenone (0.5 mg/ml stock) in DMSO or DMSO vehicle 1 time, 3 hours before harvesting organ. Confocal imaging of sliced kidney (**A**) and heart (**B**) from DHE-injected DMSO-treated control group (DMSO) and rotenone-treated group (rotenone). Rotenone treatment was initiated 30 minutes before injection with DHE (n = 3 mice per group). Original magnification, ×25. Representative immunoblot analysis and quantitative analysis of phosphorylated PDHE1a -pSer^{293} and p-AMPK in kidney (**C**, **E**, and **F**) and heart (**D**, **G**, and **H**) from DMSO-treated control and rotenone-treated mice. (n = 6 per group, $^*P < 0.05$ vs. DMSO; $^{**}P < 0.05$ vs. DMSO).

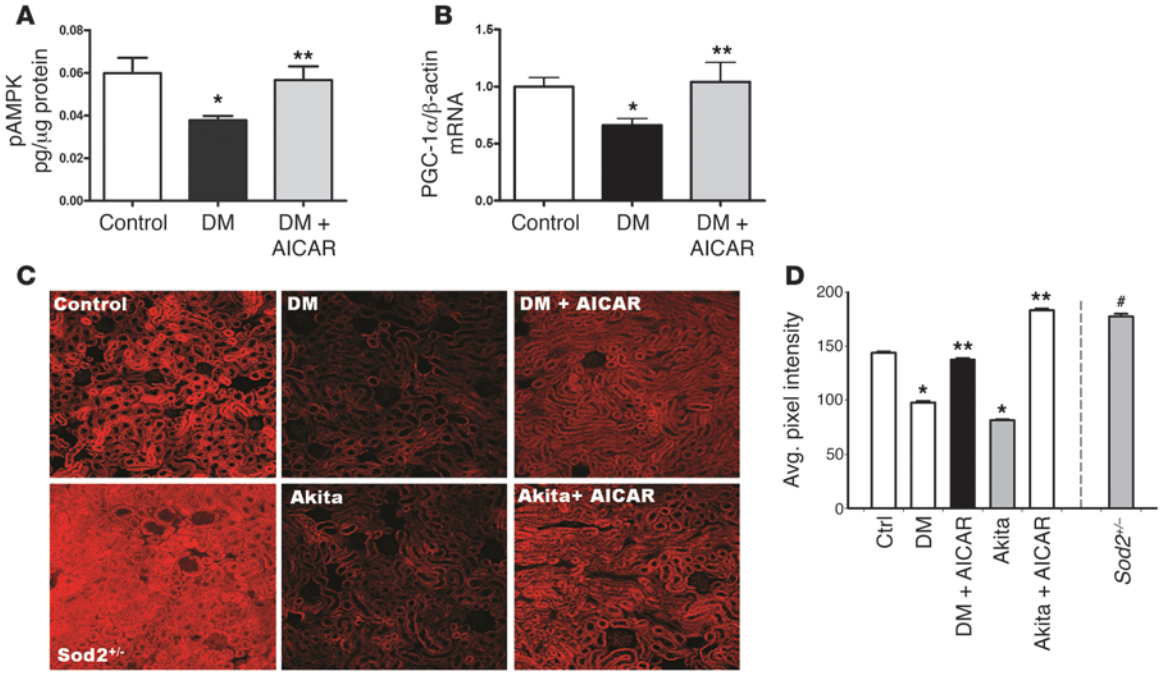

Figure 6
AICAR increases AMPK activity and PGC1α expression in the diabetic kidneys, and AMPK activation reverses superoxide production. (**A**) p-AMPK was increased in diabetic kidneys treated with AICAR ($n > 7$ per group, $^{*}P < 0.05$ vs control, $^{**}P < 0.05$ vs STZ-diabetes). (**B**) PGC1α gene expression was increased in the diabetic kidneys treated with AICAR as demonstrated by real-time PCR analysis ($n = 6$ per group, $^{*}P < 0.05$ vs. control, $^{**}P < 0.05$ vs. STZ-diabetes). (**C**) Representative confocal fluorescent images of DHE oxidation indicate that superoxide is reduced in kidneys of STZ-induced diabetic and Akita diabetic mice (AKITA) and is restored in both models by AICAR. Original magnification, ×10. *Sod2*$^{+/-}$ mice increase in DHE oxidation. (**D**) Quantification of renal superoxide in control, diabetic, *Sod2*$^{+/-}$, and diabetic mice treated with AICAR. ($n \geq 6$ per group, $^{*}P < 0.05$ vs. control; $^{**}P < 0.05$ vs. corresponding diabetic group; $^{\#}P < 0.001$ vs. other conditions).

kidneys of mice in each group and found to be reduced in the diabetic kidney and increased by AMPK activation (Figure 7, B–D). Consistent with the finding that AMPK activation leads to increased mitochondrial complex activity, there was a concomitant reduction in PDH phosphorylation (increased PDH activity) in the kidneys from AICAR-treated diabetic mice (Figure 7E and see below). AICAR treatment also resulted in a reduction of mtDNA deletion to normal levels (Figure 7F). Thus AMPK activation increased mitochondrial content and function coincident with increasing superoxide production in the diabetic kidney.

AMPK activation reduced inflammation and matrix accumulation and improved diabetic kidney disease. The main pathologic feature of diabetic kidney disease is an accumulation of matrix molecules in the glomerulus, largely driven by stimulation of TGF-β (22–24). There was an increase in glomerular fibronectin, type IV collagen, and TGF-β in the diabetic mouse glomerulus. Interestingly, concomitant with the AICAR-induced increase in superoxide production in the diabetic kidney, there was an increase in PGC1α (Figure 8, A and C) and a reduction in fibronectin (Figure 8, A and D), type IV collagen (Supplemental Figure 4A), and TGF-β (Figure 8, B and E) in the diabetic glomerulus. The most consistent clinical feature of diabetic kidney disease is an increase in the urine albumin/creatinine ratio in humans as well as in experimental models of diabetic kidney disease (25, 26). Albuminuria was increased in the diabetic mice (STZ-induced and Akita) and completely normalized by AICAR treatment (Figure 9A). Urine hydrogen peroxide (Figure 9B), glomerular 8-OHdG (Figure 9, C and D), and nitrotyrosine (Supplemental Figure 4B) as a measure of renal inflammation were markedly elevated in the diabetic mice and reduced with AMPK activation.

To further validate that AMPK is the critical enzyme responsible for regulating mitochondrial function in diabetic kidney disease, additional studies were performed with a model of progressive diabetic kidney disease (the F1 cross of DBA2J and C57BL/6J with Akita) (27, 28) and with the *Ampka2*$^{-/-}$ mice (29). Similar to the diabetic models with C57BL/6J, the F1 Akita model with diabetic kidney disease exhibited reduced renal superoxide levels. AICAR and another AMPK activator, metformin, significantly reduced albuminuria and urine hydrogen peroxide levels in the F1 diabetic mice (Supplemental Figure 5, A and B). Similar to studies in the C57BL/6J mice, there was a reduction in PDH activity and an increase in mtDNA deletions that were attenuated with AMPK activation (Supplemental Figure 5, C–E). Mice deficient in AMPKα2 exhibited elevated urine albumin and urine hydrogen peroxide levels; however, treatment with AICAR was ineffective in reducing albuminuria and urine hydrogen peroxide (Figure 9, E and F), thus demonstrating that AMPK was necessary for the beneficial effect of AICAR.

Discussion

The prevailing theory implicating mitochondrial overproduction of superoxide to explain the basis for diabetic complications has led to a multitude of studies and interventional approaches to inhibit mitochondrial superoxide production. However, the approaches used in the present study to investigate superoxide

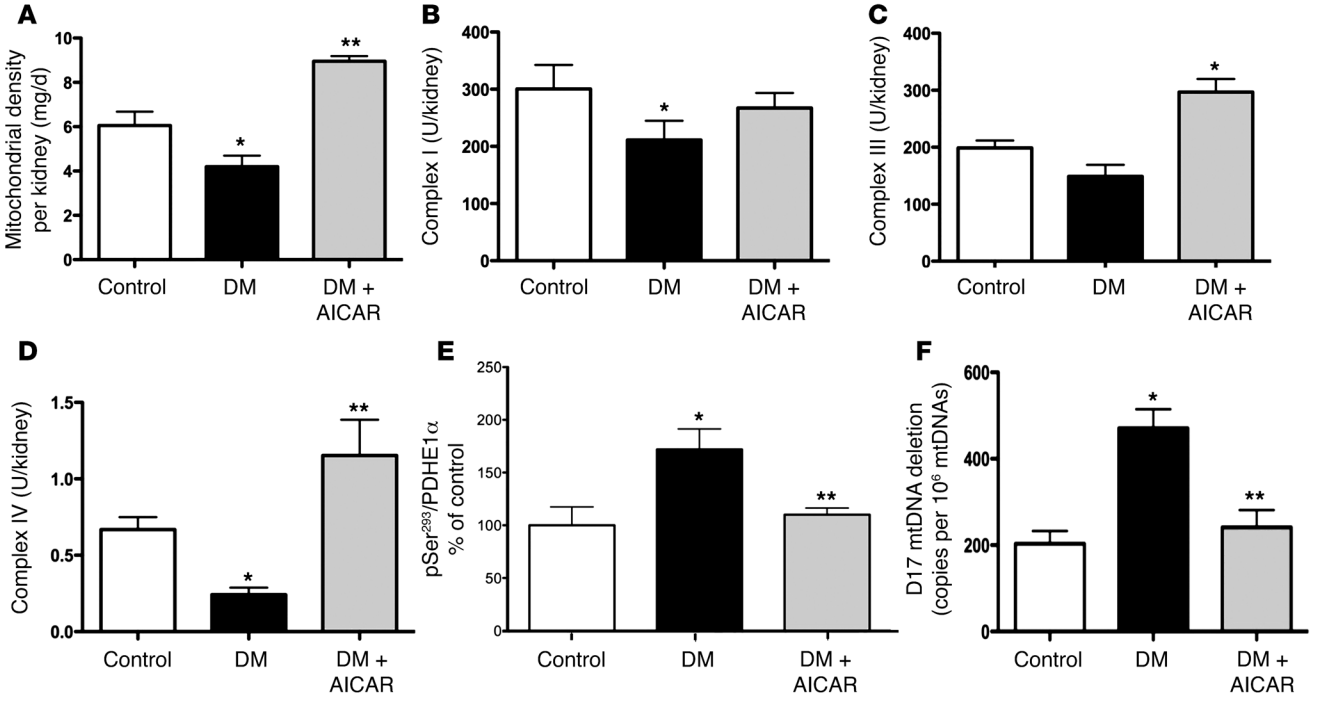

Figure 7

AMPK activation reverses diabetes-induced regulation of mitochondrial respiratory chain function, mtDNA deletion, and PDH phosphorylation. (**A**) Total mitochondrial content per kidney protein (mg/g), (**B**) complex I activity, (**C**) complex III activity, (**D**) complex IV activity, (**E**) quantitative analysis of PDH phosphorylation, and (**F**) D17 mtDNA deletion in kidney DNA measured in control, STZ-diabetic, and STZ-diabetic mice treated with AICAR (DM-AICAR). ($n \geq 6$ per group, $^{*}P < 0.05$ vs. control; $^{**}P < 0.05$ vs. corresponding diabetic group).

production in vivo led to the opposite conclusion, i.e., that there is reduced superoxide production in diabetic kidney disease and that mitochondrial activity is suppressed. The basis for the regulation of mitochondrial function is largely due to AMPK, as activation of AMPK restores mitochondrial function and superoxide production. AMPK activity is also reduced in human diabetic kidney disease, suggesting that similar pathways are operant in human diabetic nephropathy.

To put our data into context, diabetes may be viewed as a metabolic environment characterized by a surplus of calories. Mitochondria respond to the caloric availability of the cell by following 2 major pathways: anaplerosis or cataplerosis (30). In states of intermittent caloric depletion associated with increased AMPK and PGC1α activity, mitochondria pursue an anaplerosis program and consume electrons and carbons for redox regulation and oxidative phosphorylation in order to efficiently generate ATP. However, in states of sustained positive caloric balance (characterized by reduced AMPK and PGC1α), mitochondria are physiologically regulated to consume fewer electrons and oxygen, and carbon skeletons are released to the cytosol for use as building blocks for cell growth. The release of carbon skeletons from the Krebs cycle to the cytosol for protein, fat, pyrimidine, and carbohydrate synthesis is termed cataplerosis (30).The physiologic reduction of carbon flow into mitochondria under conditions of caloric excess is regulated in part by the inhibition of PDH by hyperphosphorylation, leading to reduced pyruvate entry into mitochondria (31). As diabetic kidney disease is associated with PDH hyperphosphorylation, reduced respiratory chain complex function, and reduced superoxide production, there would be a consequent reduction of carbon flow into the mitochondria. A primary reduction in mitochondrial superoxide production in the absence of high glucose (i.e., with rotenone) is sufficient to reduce AMPK and PDH activity, thus demonstrating a feedback loop to further inhibit mitochondrial function and biogenesis. In addition, a recent study found that mitochondria-derived superoxide in insulin-secreting cells promotes AMPK activity (32). A decrease in mitochondrial respiration in the presence of high glucose is called the Crabtree effect (33). Our studies demonstrate that diabetic kidney disease is characterized by the Crabtree effect, which links to AMPK activity and characteristic features of diabetic kidney disease (albuminuria and matrix accumulation) (34).

We found that in addition to the inhibition of mitochondrial respiratory chain and PDH function, diabetes resulted in a nearly 3-fold increase in mtDNA deletions in the kidney. Increases in mtDNA deletions are typically observed as a biomarker of cell stress or aging and are removed by autophagy of damaged mitochondria. We found that an increase in mtDNA deletions with diabetes was associated with reduced superoxide production. Our data are consistent with prior findings demonstrating that mtDNA deletions can be completely uncoupled from oxidative damage (35). In a mouse model of accelerated aging resulting from mtDNA deletions and caused by a mutation in the mitochondrial DNA polymerase γ (35, 36), no evidence for oxidative damage was found. Indeed, several measures of oxidative damage were actually improved despite massive amounts of mtDNA damage (35). The induction of mtDNA deletions and damage appears to be an ancient and early response to many kinds of cellular metabolic stress (37) and may be an intrinsic feature of the innate immune (38), or cellular "danger" response (37, 39).

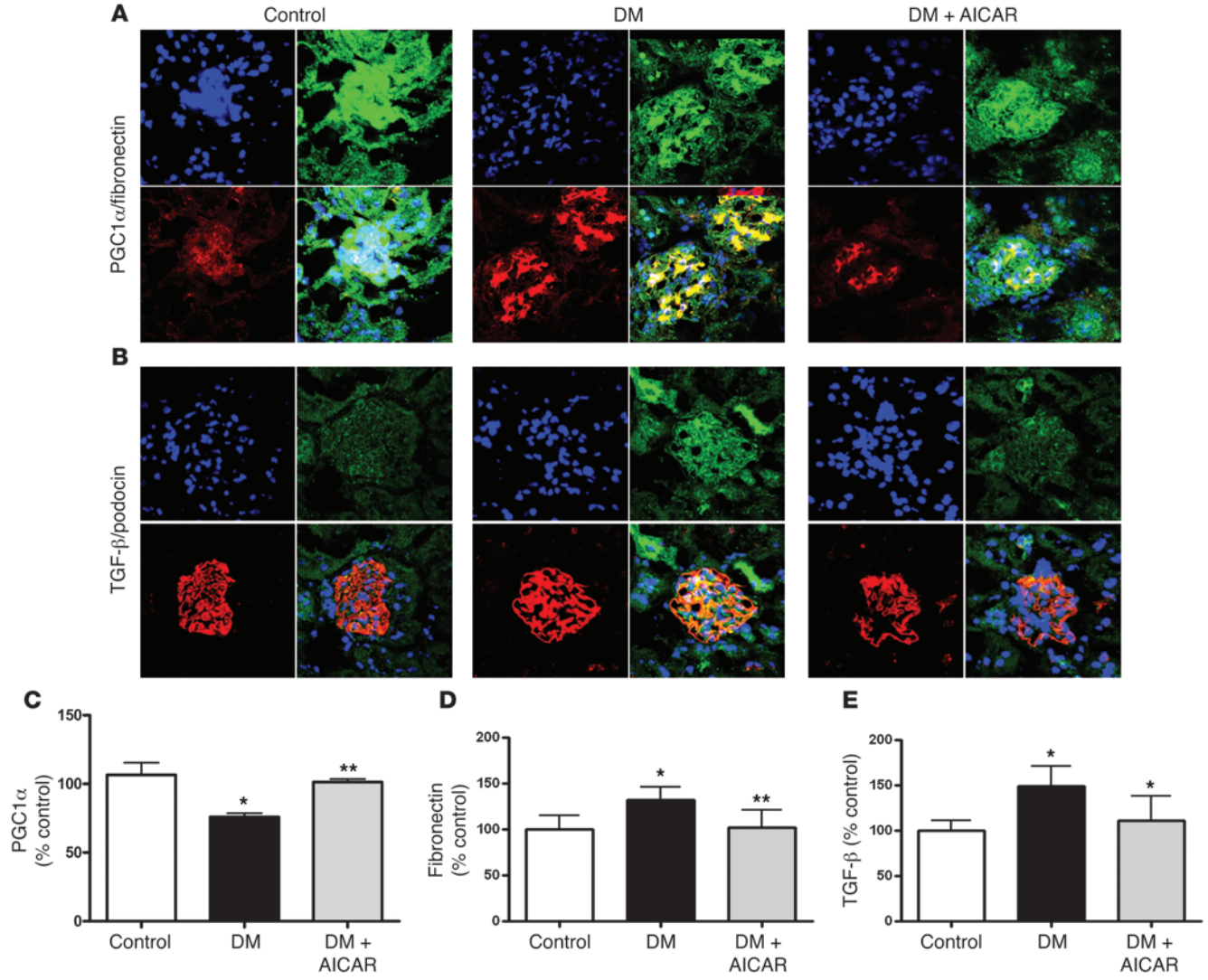

Figure 8

AMPK activation increases PGC1α and reduces fibronectin and TGF-β. (**A**) AICAR treatment increased PGC1α (green) in the diabetic kidney concurrently with a reduction in glomerular fibronectin (red). (**B**) AICAR treatment reduced glomerular TGF-β (green) in diabetic kidneys (podocin staining in red). Confocal images representative of $n = 3$ mice per group. Original magnification, ×63. Semiquantitative data of immunostaining of PGC1α (**C**), fibronectin (**D**), and TGF-β (**E**) in glomeruli. ($n \geq 6$ per group, $^{*}P < 0.05$ vs control; $^{**}P < 0.05$ vs corresponding diabetic group).

In the present study, we demonstrated that stimulation of mitochondrial structure and function via AMPK activation led to an increase in superoxide production and a reduction in parameters of diabetic kidney disease. In contrast to the prediction of the prevailing theories regarding the deleterious consequences of mitochondrial superoxide production (2), we found that the increase in mitochondrial function and superoxide production was associated with a beneficial reduction of pathophysiologic characteristics of diabetic kidney disease (i.e., glomerular matrix, TGF-β, and albuminuria). This is consistent with the findings that some types of ROS may be protective and inhibit inflammation, as shown in autoimmune disorders such as rheumatoid arthritis, multiple sclerosis, thyroiditis, and type 1 diabetes (40). The associated improvement in the parameters of diabetic kidney disease with increased mitochondrial function and superoxide production demonstrates that enhanced mitochondrial activity is not a necessary contributor to diabetic kidney disease.

There are similarities with respect to diabetic kidney and diabetic heart disease, in that both conditions are associated with an increase in matrix accumulation and TGF-β production (41–44). Our studies suggest that there could be a similar response in the heart and kidney to diabetes, with respect to mitochondrial superoxide production; however, further studies are required to comprehensively evaluate mitochondrial function in diabetic heart disease and in relation to matrix accumulation. It is likely that mitochondrial superoxide production plays an important signaling role and is necessary for normal physiologic intracellular communication. Further studies to examine the downstream consequences of short- and long-term activation of AMPK and mitochondrial biogenesis in the context of diabetic complications are warranted. Interestingly, we found that human diabetic kidney disease is also characterized by reduced mitochondrial function based on urine metabolomics and kidney biopsy studies (45).

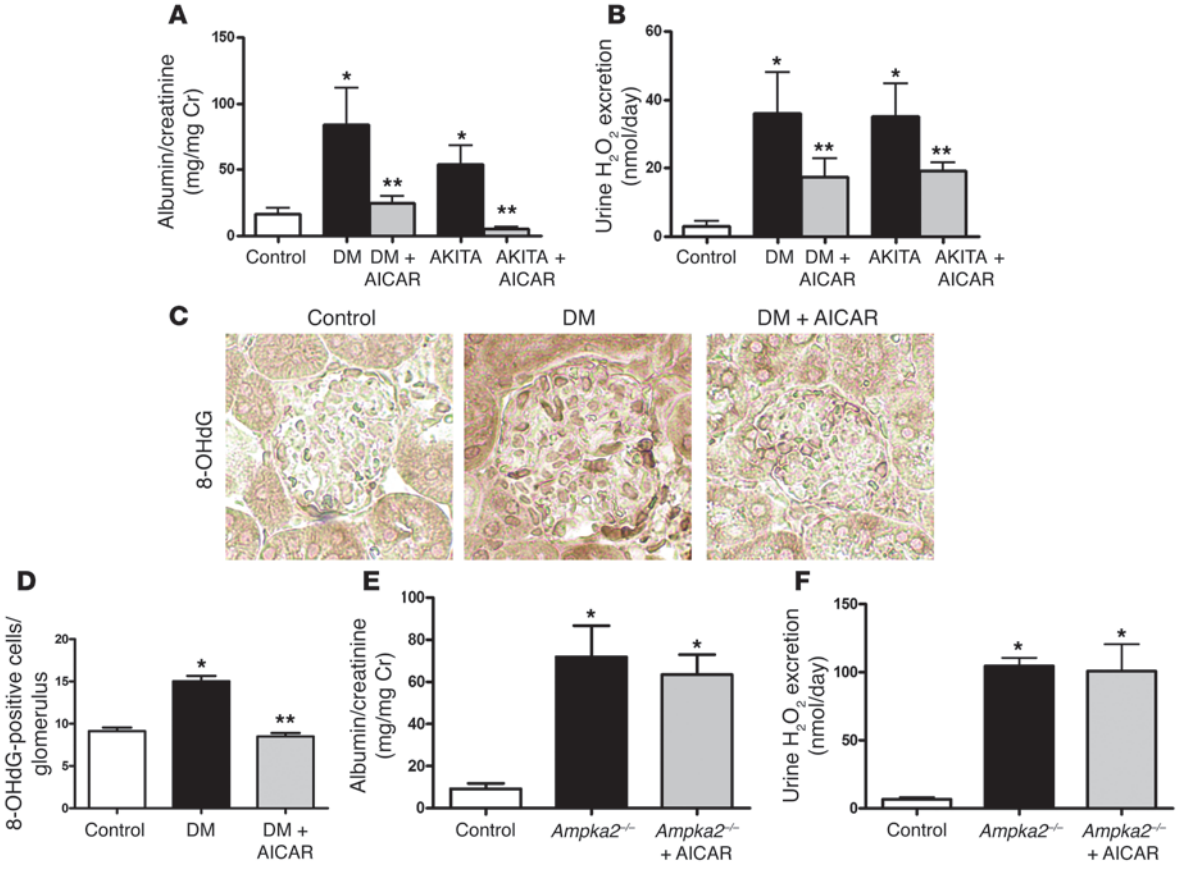

Figure 9

AMPK activation reduces urine albumin, urine hydrogen peroxide, and glomerular 8-OHdG. AICAR reduced the urine albumin/creatinine ratio (**A**) and hydrogen peroxide (H_2O_2) excretion (**B**) in the diabetic mice. ($n \geq 8$ per group, $^*P < 0.05$ vs. control; $^{**}P < 0.05$ vs. corresponding diabetic group). (**C**) Glomerular 8-OHdG content was significantly increased in the diabetic groups and significantly reduced by AICAR treatment by immunoperoxidase staining. Original magnification, ×40. (**D**) Quantification of 8-OHdG–positive cells per glomerulus. $n = 20$ glomeruli from each mouse kidney; 3 mice per group. $^*P < 0.001$ vs. control; $^{**}P < 0.001$ vs. DM. *Ampka2*$^{-/-}$ mice underwent urine collections and albumin/creatinine ratio (**E**) and hydrogen peroxide excretion (**F**) are shown ($n = 6$ per group, $P < 0.05$ vs. control).

Therefore, in addition to glycemic and blood pressure control, restoration of mitochondrial structure, function, and signaling may be novel ways to improve diabetic kidney disease and prevent the decline in organ function.

Methods

Animal studies. All studies involving mice were approved by the UCSD Institutional Animal Care and Use Committee. C57BL/6J mice were made diabetic by a low dose STZ protocol (AMDCC). The *Sod2*$^{+/-}$ mice were purchased from Jackson Laboratories and studied at the University of Michigan. Akita mice were derived from a cross between C57BL/6J-*Ins2*^{Akita} males and C57BL/6J females or an F1 cross between male Akita C57BL/6J-*Ins2*^{Akita} and female DBA (all purchased from Jackson Laboratories). *Ampka2*$^{-/-}$ mice were from Benoit Viollet's lab and sent courtesy of Jay Chung at the NIH. In the interventional study with AICAR, diabetic and control mice were randomized to AICAR (500 mg/kg, i.p. daily), or metformin (150 mg/kg i.p. daily) (Sigma-Aldrich) was given to the F1 (DBA/2J × C57BL/6J) -*Ins2*^{Akita} diabetic mice for a period of 2 weeks. Each experimental protocol consisted of 4 groups, wild-type control, wild-type diabetic (STZ treated), transgenic control, and transgenic diabetic (STZ treated). Each group contained 10 animals unless otherwise indicated. Tissues were harvested 24 weeks after induction of diabetes.

Urine albumin and hydrogen peroxide measurements. The urine albumin and creatinine were measured with a mouse Albuwell ELISA kit and a Creatinine Companion kit (Exocell). As an index of oxidative stress, urine samples were also analyzed for hydrogen peroxide by Amplex red assay (Invitrogen) according to the manufacturer's protocol.

Human subjects. Slides of normal kidney tissue and diabetic kidney disease from patients were obtained from Agnes Fogo from archived tissue samples.

Superoxide measurement. For measurement of superoxide generation, diabetic and control mice were administered DHE (50 mg/kg) by i.p. injection as described (6, 8). For live animal imaging, anesthetized mice were administered FITC-inulin 30 minutes before being placed in the eXplore Optix-MX2 live animal scanner (Advanced Research Technologies Inc.). Each mouse was individually scanned using a 470-nm excitation laser and a 590-nm long-pass detection filter. For confocal imaging of DHE oxidation in postmortem slices, DHE-injected mice were anesthetized, perfused with cold saline followed by 4% paraformaldehyde, and dissected. Mounted tissue slices were imaged on a LSM510 Meta multiphoton laser confocal microscope (Karl Zeiss Inc.). To demonstrate that DHE was not handled differently in the diabetic kidney, [^{14}C]-labeled DHE was synthesized using 1 mCi [^{14}C]-ring benzoic acid, [ring-u-14C] (Chemdepo Inc.) to produce [^{14}C]-labeled ethidium as described (46). This underwent reduction to [^{14}C]-DHE using sodium borohydride in water as

described (47). After column purification, purity and identity were confirmed by both LC-MS and by HPLC/diode array spectroscopy. Mice were then injected with 50 Ci ^{14}C-DHE and euthanized 1 hour after injection; the kidneys were harvested, weighed, and solubilized and the amount of [^{14}C]-DHE determined on a Beckman Coulter scintillation counter. For rotenone treatment, C57BL/6J mice were injected i.p. with either 1 μg/g rotenone (0.5 mg/ml stock) in DMSO or DMSO vehicle 3 hours before harvesting organs. For tissue confocal images, mice were administered rotenone 30 minutes before receiving DHE (50 mg/kg) by i.p. injection. For EPR studies, control and diabetic mice were euthanized by inhaled isoflurane and then underwent intracardial perfusion with cold BIOPS solution. The kidneys were rapidly removed and placed in cold BIOPS. The tissue homogenate was injected into the EPR cavity through a gas-permeable Teflon tube. These studies were carried out in a MiniScope MS200 Benchtop EPR Spectrometer (Magnettech), which is designed to allow tight control of pO_2 and temperature. Calibration of EPR signal intensity to paramagnetic species, e.g., superoxide anion, were carried out using the stable radical, 4-hydroxy-TMPO.

Mitochondrial enzymatic activity and DNA analysis. Mitochondrial isolation and complex activity were performed in mice after euthanasia by cervical dislocation. Tissues were rapidly dissected and placed in ice-cold BIOPS before mitochondrial isolation. Kidney mitochondria for respiratory chain enzymology were isolated by a modification of previously published methods from our lab (48). The enzymatic activity of mitochondrial complex I was measured as NADH:CoQ1 oxidoreductase activity (49). Complex III was measured as decylubiquinol:cytochrome *c* reductase activity (50). Complex IV was measured as cytochrome *c* oxidase activity (49). Mitochondrial DNA analysis was performed from total DNA extracted from kidneys. Real-time qPCR was performed as previously described (51). All assays included titration curves of positive controls, which consisted of dilutions of a cloned fragment of mouse mtDNA that contains the D17 deletion, a cloned fragment of the mouse mtDNA ND4 region, and a nuclear DNA copy number control consisting of a cloned fragment of mouse β-actin gene.

Measurement of mitochondrial ROS release. Release of hydrogen peroxide from kidney mitochondria was measured using Amplex Red Hydrogen Peroxide/Peroxidase Assay Kit (Invitrogen). Assay protocol was optimized to make it suitable for real-time monitoring of ROS release from intact mitochondria, as follows. Mitochondria (0.5 mg/ml) were incubated in mitochondrial assay medium (125 mM KCl, 2 mM potassium phosphate, 20 mM HEPES-KOH, pH 7.0). Detection system consisted of 0.15 unit/ml horseradish peroxidase and 5 μM Amplex Red. Increase in fluorescence was monitored over time at $\lambda_{ex}/\lambda_{em}$ = 563/587 using LS50B spectrofluorometer (PerkinElmer). Assay was calibrated by sequential additions of standard additions of hydrogen peroxide in the range 0.1–4 μM. Reverse electron transport–mediated ROS production was assayed in the presence of 10 mM succinate followed by addition of uncoupler FCCP (0.5 μM). Then 5 mM glutamate plus 5 mM malate were used as respiratory substrates to assess ROS production under conditions of direct electron flow, in the presence or absence or complex I inhibitor rotenone (2 μM).

Immunofluorescence. Immunofluorescence staining was performed on frozen kidney sections that were fixed in 4% paraformaldehyde, as previously described (52). The following primary antibodies were used for immunofluorescence staining: rabbit polyclonal anti-PGC1α (Santa Cruz Biotechnology Inc.), goat polyclonal anti-fibronectin (BD Biosciences), rabbit polyclonal anti–TGF-β (pan-specific; Santa Cruz Biotechnology Inc.), rabbit monoclonal anti–p-AMPKα (Thr172) (Cell Signaling Technology), and goat polyclonal anti-podocin (Santa Cruz Biotechnology Inc.). The following secondary antibodies were used for immunofluorescence staining: Alexa Fluor 488 goat anti-mouse (Invitrogen), Alexa Fluor 594 goat anti-rabbit (Invitrogen), and Alexa Fluor 488 donkey anti-goat (Invitrogen). Images were visualized under ×25, ×63, and ×100 objectives using a confocal LSM 510 microscope (Zeiss). For each antibody, there were at least 5 mice per group.

Immunohistochemistry. Immunostaining for p-AMPK (The172) (Cell Signaling) was performed in paraffin-embedded human kidney sections and visualized using chromogen diaminobenzidine (DAB) (Vector Labs). Positive staining was assessed on images taken at ×400 magnification using a semiquantitative scoring method. Briefly, a score of 0–4 was assigned to glomeruli based on intensity of staining and amount of total glomerular area that was stained on 20 glomeruli randomly imaged from 10 normal samples and 18 glomeruli from 9 diabetic samples.

RNA isolation and real-time qPCR. Total RNA was isolated from kidney cortex using TriZOL reagent (Invitrogen) and real-time qPCR was performed as previously described (53). The primers for PGC1α was as follows: forward, 5′-TGATAAACTGAGCTACCCTTG-3′; reverse, 5′-ACACTGAGTCTCGACACGG-3′, and β-actin as a housekeeping gene.

Immunoblotting. Immunoblotting was performed as described previously (54). Primary antibodies used rabbit anti–p-PDH (pSer^{293}) (EMD Chemicals Inc.) and rabbit polyclonal anti-PDHE1α (Invitrogen). The blots were visualized on a phosphorimager (Molecular Dynamics Storm PhosphorImager), and the image analysis was performed using ImageQuant TL Software (Amersham Biosciences).

AMPKα activity. The level of activated AMPKα1 in renal cortex tissue was determined by a sandwich ELISA to measure AMPKα1 phosphorylated at T174 (R&D Systems) according to the manufacturer's protocol.

Statistics. Results are presented as mean values ± SEM. The level for statistical significance was defined as $P < 0.05$. Analyses were carried out using Graph Pad Prism Software version 4.03. Differences between data groups were evaluated for significance using independent *t* test or the Mann-Whitney test of data, as appropriate, or 1-way ANOVA and Newman-Keuls for multiple comparisons.

Study approval. All studies involving mice were approved by the Institutional Animal Care and Use Committee (IACUC) at UCSD and the University of Michigan Medical School. Human samples were obtained from archived tissue under an approved IRB protocol and were deidentified.

Acknowledgments

The authors would like to acknowledge the support of the Juvenile Diabetes Research Foundation (JDRF) (to K. Sharma and L.L. Dugan) and the NIH and the VA for these studies (DP3DK094352, U01DK076133 to K. Sharma; R01DK053867 to K. Sharma; VA Merit to K. Sharma;R21AG030320 and R01AG033679 to L.L. Dugan). We also acknowledge support from the Christini Fund, the Wright Foundation, and the Lennox Foundation (to R.K. Naviaux) as well as the Larry L. Hillblom Foundation (to L.L. Dugan). We thank Robert Henry, Chris Glass, and Nigel Calcutt of UCSD for their critical review and helpful comments of the manuscript.

Received for publication August 13, 2012, and accepted in revised form August 8, 2013.

Address correspondence to: Young-Hyun You or Kumar Sharma, Center for Renal Translational Medicine, Division of Nephrology, Department of Medicine, Stein Research Building, 9501 Gilman Drive #0711, University of California San Diego, La Jolla, California 92093-0711, USA. Phone: 858.822.0875; Fax: 858.822.7483; E-mail: yoyou@ucsd.edu (Y.-H. You). Phone: 858.822.0860, Fax: 858.822.7483; E-mail: kusharma@ucsd.edu (K. Sharma).

1. Nishikawa T, et al. Normalizing mitochondrial superoxide production blocks three pathways of hyperglycaemic damage. *Nature*. 2000; 404(6779):787–790.
2. Brownlee M. Biochemistry and molecular cell biology of diabetic complications. *Nature*. 2001; 414(6865):813–820.
3. DeRubertis F, Craven P, Melhem M, Salah E. Attenuation of renal injury in db/db mice overexpressing superoxide dismutase: evidence for reduced superoxide-nitric oxide interaction. *Diabetes*. 2004; 53(3):762–768.
4. Lin CL, et al. Superoxide destabilization of beta-catenin augments apoptosis of high-glucose-stressed mesangial cells. *Endocrinology*. 2008;149(6):2934–2942.
5. Rinaldi M, Moroni P, Paape MJ, Bannerman DD. Evaluation of assays for the measurement of bovine neutrophil reactive oxygen species. *Vet Immunol Immunopathol*. 2007;115(1–2):107–125.
6. Hall DJ, Han SH, Chepetan A, Inui EG, Rogers M, Dugan LL. Dynamic optical imaging of metabolic and NADPH oxidase-derived superoxide in live mouse brain using fluorescence lifetime unmixing. *J Cereb Blood Flow Metab*. 2012;32(1):23–32.
7. Quick KL, Dugan LL. Superoxide stress identifies neurons at risk in a model of ataxia-telangiectasia. *Ann Neurol*. 2001;49(5):627–635.
8. Behrens MM, et al. Ketamine-induced loss of phenotype of fast-spiking interneurons is mediated by NADPH-oxidase. *Science*. 2007;318(5856):1645–1647.
9. Sarre C, et al. Risk factors for Psoroptes ovis mange on Belgian Blue farms in Northern Belgium. *Vet Parasitol*. 2012;190(1–2):216–221.
10. Han Y, Tuccio B, Lauricella R, Villamena FA. Improved spin trapping properties by beta-cyclodextrin-cyclic nitrone conjugate. *J Org Chem*. 2008; 73(18):7108–7117.
11. Frejaville C, et al. 5-(Diethoxyphosphoryl)-5-methyl-1-pyrroline N-oxide: a new efficient phosphorylated nitrone for the in vitro and in vivo spin trapping of oxygen-centered radicals. *J Med Chem*. 1995;38(2):258–265.
12. Ali SS, et al. A biologically effective fullerene (C(60)) derivative with superoxide dismutase mimetic properties. *Free Radic Biol Med*. 2004;37(8):1191–1202.
13. Ali SS, Hsiao M, Zhao HW, Dugan LL, Haddad GG, Zhou D. Hypoxia-adaptation involves mitochondrial metabolic depression and decreased ROS leakage. *PLoS One*. 20012;7(5):e36801.
14. Dugan LL, et al. IL-6 mediated degeneration of forebrain GABAergic interneurons and cognitive impairment in aged mice through activation of neuronal NADPH oxidase. *PLoS ONE*. 2009; 4(5):e5518.
15. Ali SS, Hardt JI, Dugan LL. SOD activity of carboxyfullerenes predicts their neuroprotective efficacy: a structure-activity study. *Nanomedicine*. 2008; 4(4):283–294.
16. Sharma K, et al. Adiponectin regulates albuminuria and podocyte function in mice. *J Clin Invest*. 2008; 118(5):1645–1656.
17. Rardin MJ, Wiley SE, Naviaux RK, Murphy AN, Dixon JE. Monitoring phosphorylation of the pyruvate dehydrogenase complex. *Anal Biochem*. 2009; 389(2):157–164.
18. Decleves AE, et al. AMPK mediates the initiation of kidney disease induced by a high-fat diet. *J Am Soc Nephrol*. 2011;22(10):1846–1855.
19. Lee MJ, et al. A role for AMP-activated protein kinase in diabetes-induced renal hypertrophy. *Am J Physiol Renal Physiol*. 2007;292(2):F617–F627.
20. Deng YT, Huang HC, Lin JK. Rotenone induces apoptosis in MCF-7 human breast cancer cell-mediated ROS through JNK and p38 signaling. *Mol Carcinog*. 2010;49(2):141–151.
21. Lai CF, Shao JS, Behrmann A, Krchma K, Cheng SL, Towler DA. TNFR1-activated reactive oxidative species signals up-regulate osteogenic Msx2 programs in aortic myofibroblasts. *Endocrinology*. 2012; 153(8):3897–3910.
22. Ziyadeh FN, Sharma K, Ericksen M, Wolf G. Stimulation of collagen gene expression and protein synthesis in murine mesangial cells by high glucose is mediated by activation of transforming growth factor-β. *J Clin Invest*. 1994;93(2):536–542.
23. Sharma K, Guo J, Jin Y, Ziyadeh FN. Neutralization of TGF-β by anti-TGF-β antibody attenuates kidney hypertrophy and the enhanced extracellular matrix gene expression in STZ-induced diabetic mice. *Diabetes*. 1996;45(4):522–530.
24. Ziyadeh F, et al. Long-term prevention of renal insufficiency excess matrix gene expression and glomerular mesangial matrix expansion by treatment with monoclonal antitransforming growth factor-b antibody in db/db diabetic mice. *Proc Natl Acad Sci U S A*. 2000;97(14):8015–8020.
25. Viberti GC, Hill RD, Jarrett RJ, Argyropoulos A, Mahmud U, Keen H. Microalbuminuria as a predictor of clinical nephropathy in insulin-dependent diabetes mellitus. *Lancet*. 1982;1(8287):1430–1432.
26. Hellemons ME, et al. Validity of biomarkers predicting onset or progression of nephropathy in patients with type 2 diabetes. *Diabet Med*. 2012; 29(5):567–577.
27. Brosius FC 3rd, et al. Mouse models of diabetic nephropathy. *J Am Soc Nephrol*. 2009; 20(12):2503–2512.
28. Gurley SB, et al. Influence of genetic background on albuminuria and kidney injury in Ins2(+/C96Y) (Akita) mice. *Am J Physiol Renal Physiol*. 2010; 298(3):F788–F795.
29. Viollet B, et al. Physiological role of AMP-activated protein kinase (AMPK): insights from knockout mouse models. *Biochem Soc Trans*. 2003; 31(pt 1):216–219.
30. Owen OE, Kalhan SC, Hanson RW. The key role of anaplerosis and cataplerosis for citric acid cycle function. *J Biol Chem*. 2002;277(34):30409–30412.
31. Patel MS, Korotchkina LG. Regulation of the pyruvate dehydrogenase complex. *Biochem Soc Trans*. 2006;34(Pt 2):217–222.
32. Sarre A, Gabrielli J, Vial G, Leverve XM, Assimacopoulos-Jeannet F. Reactive oxygen species are produced at low glucose and contribute to the activation of AMPK in insulin-secreting cells. *Free Radic Biol Med*. 2012;52(1):142–150.
33. Ibsen KH. The Crabtree effect: a review. *Cancer Res*. 1961;21:829–841.
34. Naviaux RK, et al. Retained features of embryonic metabolism in the adult MRL mouse. *Mol Genet Metab*. 2009;96(3):133–144.
35. Kujoth GC, et al. Mitochondrial DNA mutations, oxidative stress, and apoptosis in mammalian aging. *Science*. 2005;309(5733):481–484.
36. Klaus A, Polge C, Zorman S, Auchli Y, Brunisholz R, Schlattner U. A two-dimensional screen for AMPK substrates identifies tumor suppressor fumarate hydratase as a preferential AMPKalpha2 substrate. *J Proteomics*. 2012;75(11):3304–3313.
37. Zhang Q, et al. Circulating mitochondrial DAMPs cause inflammatory responses to injury. *Nature*. 2010;464(7285):104–107.
38. Suliman HB, Welty-Wolf KE, Carraway MS, Schwartz DA, Hollingsworth JW, Piantadosi CA. Toll-like receptor 4 mediates mitochondrial DNA damage and biogenic responses after heat-inactivated E. coli. *FASEB J*. 2005;19(11):1531–1533.
39. Naviaux RK. Metabolic features of the cell danger response [published online ahead of print August 24, 2013]. *Mitochondrion*. doi:10.1016/j.mito.2013.08.006.
40. Hultqvist M, Olsson LM, Gelderman KA, Holmdahl R. The protective role of ROS in autoimmune disease. *Trends Immunol*. 2009;30(5):201–208.
41. Wilson P, Drennon K, Tannock LR. Regulation of vascular proteoglycan synthesis by metabolic factors associated with diabetes. *J Investig Med*. 2007; 55(1):18–25.
42. Little PJ, Tannock L, Olin KL, Chait A, Wight TN. Proteoglycans synthesized by arterial smooth muscle cells in the presence of transforming growth factor-beta1 exhibit increased binding to LDLs. *Arterioscler Thromb Vasc Biol*. 2002;22(1):55–60.
43. Cagliero E, Roth T, Roy S, Lorenzi M. Characteristics and mechanisms of high-glucose-induced overexpression of basement membrane components in cultured human endothelial cells. *Diabetes*. 1991;40(1):102–110.
44. Spiro MJ, He Q, D'Autilia ML. Effect of high glucose on formation of extracellular matrix components by cultured rat heart endothelial cells. *Diabetologia*. 1995;38(4):430–436.
45. Sharma K, et al. Metabolomics reveals signature of mitochondrial dysfunction in diabetic kidney disease [published online ahead of print October 10, 2013]. *J Am Soc Nephrol*. doi:10.1681/ASN.2013020126.
46. De Nobrega Bastos R, Mahler HR. A synthesis of labeled ethidium bromide. *Arch Biochem Biophys*. 1974;160(2):643–646.
47. Thomas G, Roques B. Proton magnetic resonance studies of ethidium bromide and its sodium borohydride reduced derivative. *FEBS Lett*. 1972; 26(1–2):169–175.
48. Hoppel CL, Kerner J, Turkaly P, Turkaly J, Tandler B. The malonyl-CoA-sensitive form of carnitine palmitoyltransferase is not localized exclusively in the outer membrane of rat liver mitochondria. *J Biol Chem*. 1998;273(36):23495–23503.
49. Taylor RWT. Laboratory diagnosis of mitochondrial disease. In: Applegarth DA, Dimmick JE, Hall JG, eds. *Organelle Diseases: Clinical Features, Diagnosis, Pathogenesis, and Management*. London, United Kingdom: Chapman and Hall Medical; 1997:341–350.
50. Barrientos A. In vivo and in organello assessment of OXPHOS activities. *Methods*. 2002;26(4):307–316.
51. Tanhauser SM, Laipis PJ. Multiple deletions are detectable in mitochondrial DNA of aging mice. *J Biol Chem*. 1995;270(42):24769–24775.
52. Agrawal YK, Sharma KR. Speciation, liquid-liquid extraction, sequential separation, preconcentration, transport and ICP-AES determination of Cr(III), Mo(VI) and W(VI) with calix-crown hydroxamic acid in high purity grade materials and environmental samples. *Talanta*. 2005;67(1):112–120.
53. Zhu Y, Casado M, Vaulont S, Sharma K. Role of upstream stimulatory factors in regulation of renal transforming growth factor-beta1. *Diabetes*. 2005; 54(7):1976–1984.
54. Sharma K, et al. Involvement of transforming growth factor-beta in regulation of calcium transients in diabetic vascular smooth muscle cells. *Am J Physiol Renal Physiol*. 2003;285(6):F1258–F1270.